J Biol Inorg Chem (2003) 8: 540–548
DOI 10.1007/s00775-003-0443-x

ORIGINAL ARTICLE

**David Aragão · Sofia Macedo
Edward P. Mitchell · Célia V. Romão
Ming Y. Liu · Carlos Frazão · Lígia M. Saraiva
António V. Xavier · Jean LeGall
Walter M.A.M. van Dongen · Wilfred R. Hagen
Miguel Teixeira · Maria A. Carrondo · Peter Lindley**

Reduced hybrid cluster proteins (HCP) from *Desulfovibrio desulfuricans* ATCC 27774 and *Desulfovibrio vulgaris* (Hildenborough): X-ray structures at high resolution using synchrotron radiation

Received: 22 November 2002 / Accepted: 14 January 2003 / Published online: 15 February 2003

Abstract The hybrid cluster proteins from the sulfate reducing bacteria *Desulfovibrio desulfuricans* ATCC 27774 (*Dd*) and *Desulfovibrio vulgaris* strain Hildenborough (*Dv*) have been isolated and crystallized anaerobically. In each case, the protein has been reduced with dithionite and the crystal structure of the reduced form elucidated using X-ray synchrotron radiation techniques at 1.25 Å and 1.55 Å resolution for *Dd* and *Dv*, respectively. Although the overall structures of the proteins are unchanged upon reduction, there are significant changes at the hybrid cluster centres. These include significant movements in the position of the iron atom linked to the persulfide moiety in the oxidized as-isolated proteins and the sulfur atom of the persulfide itself. The nature of these changes is described and the implications with respect to the function of hybrid cluster proteins are discussed.

Electronic Supplementary Material Supplementary material is available for this article if you access the article at http://dx.doi.org/10.1007/s00775-003-0443-x. A link in the frame on the left on that page takes you directly to the supplementary material.

Keywords *Desulfovibrio desulfuricans* · *Desulfovibrio vulgaris* · High-resolution X-ray structures · Hybrid cluster proteins · Reduced forms

Abbreviations *Dd*: *Desulfovibrio desulfuricans* ATCC 27774 · *Dv*: *Desulfovibrio vulgaris* strain Hildenborough · DTN: dithionite anion, S_2O4^{2-} · GOL: 1,2,3-trihydroxypropane (glycerol) · HCP: hybrid cluster protein, formerly known as prismane · MES: 2-(*N*-morpholino)ethanesulfonic acid PEG: poly(ethylene glycol)

Electronic Supplementary Material Supplementary material is available for this article if you access the article at http://dx.doi.org/10.1007/s00775-003-0443-x. A link in the frame on the left on that page takes you directly to the supplementary material.

This paper is dedicated to the memory of Jean LeGall who died on 1 March 2003.

D. Aragão · S. Macedo · C.V. Romão · C. Frazão
L.M. Saraiva · A.V. Xavier · M. Teixeira
M.A. Carrondo · P. Lindley (✉)
Instituto de Tecnologia Química e Biológica,
Universidade Nova de Lisboa, Av. República,
Apartado 127, 2781-901 Oeiras, Portugal
E-mail: lindley@itqb.unl.pt
Tel.: +351-214-469262
Fax: +351-214-413969

D. Aragão · S. Macedo · E.P. Mitchell · P. Lindley
European Synchrotron Radiation Facility,
BP 220 38043 Cedex, Grenoble , France

M.Y. Liu · J. LeGall
Department of Biochemistry, University of Georgia,
Athens, GA, 30602, USA

W.M.A.M. van Dongen
Department of Biochemistry, Wageningen University,
Dreijenlaan 3, 6703 HA Wageningen, The Netherlands

W.R. Hagen
Kluyver Department of Biotechnology,
Delft University of Technology, Julianalaan 67,
2628 BC Delft, The Netherlands

Introduction

Genes encoding hybrid cluster proteins (HCPs) have been identified in a large number of prokaryotes, including archaea and bacteria, both strict anaerobic and facultative anaerobic, as well as in eukaryotic protozoa. No specific function has yet been assigned to this family of proteins, although its involvement in the biological nitrogen cycle [1, 2] and in protection against oxidative stress [4] has been proposed. The similarity of the hybrid cluster in HCPs to the nickel-containing cluster present in the catalytic domain of the carbon monoxide

dehydrogenase from *Carboxydothermus hydrogenoformans* [5] has also been noted.

In previous structural studies [6, 7, 8] it has been shown that the HCPs from the sulfate reducing bacteria, *Dd* and *Dv*, in the as-isolated oxidized form, contain an unusual iron-sulfur cluster, whose structure appears to be independent of whether the proteins are isolated aerobically or anaerobically. This hybrid cluster is located at the interface of the three domains comprising the HCP and some 11–12 Å distant from a $[4Fe\text{-}4S]^{2+/+}$ cubane cluster which is located near the outside of the molecule at the N-terminus in domain 1. In the as-isolated protein, the hybrid cluster can be considered as being derived from a cube, but with an iron atom, Fe7, at one corner peeled back: see Fig. 1a. It is bound to the protein by seven amino acid residues lying at the interfaces of the three domains, so that:

1. Fe5 and Fe6, linked to the protein by Cys427 (Cys434 in *Dv*) and Cys308 (Cys312 in *Dv*), respectively, together with S5 and S6 form a [2Fe-2S] moiety that constitutes a face of the cube.
2. Fe8 lies at another corner of the cube, linked to the protein by Glu487 (Glu494), but is also bound to S6 of the [2Fe-2S] moiety and a persulfide moiety at Cys399 (Cys406).
3. Fe7, linked to the protein by His240 (His 244), Glu264 (Glu268) and Cys452 (Cys 459), can be considered as the fourth corner of the cube peeled away so that it lies close to the diagonal of the face formed by Fe5, S6 and Fe8 that bisects the two iron atoms.

Fig. 1 **a** A model representation of the hybrid cluster in the as-isolated oxidized form, prepared anaerobically, of *Dv* (unpublished results), showing the bridging oxygen atoms O8 (bridging Fe6 and Fe8) and O9 (bridging Fe7 and Fe8). The moiety X is also represented as an oxygen atom bridging Fe5 and Fe7. Residues Cys434 and Cys312 bound to Fe5 and Fe6, respectively, have been omitted for clarity. **b** Electron density at the hybrid cluster in the as-isolated oxidized form of *Dd* ([8] PDB ID 1GNL) showing the persulfide moiety at Fe8. The contour level is 1.0 rms in a SigmaA-weighted $2|F_o| - |F_c|$ Fourier synthesis. This is a different orientation to **a** and Fe7 and its environment have been omitted for clarity

The Fe-Fe separations range between 2.8 Å and 5.1 Å and the hybrid cluster contains both μ-S and μ-O bridges between pairs of iron atoms. Thus, O8 bridges Fe6 and Fe8, and O9 bridges Fe7 and Fe8. A further moiety, X, appears to bridge Fe5 and Fe7 and in this case the environments of the iron atoms can be described as distorted tetrahedral for Fe5 and Fe6 but distorted trigonal bipyramidal for Fe7. The coordination of Fe8 is distorted trigonal bipyramidal, but if X is also considered, it becomes distorted octahedral. In the oxidized forms of the HCP from *Dd* and *Dv*, X has been assigned as an oxygen atom on the basis of resonance Raman studies, with two possible positions in the *Dv* structure.

In the crystalline state it is possible to reduce the HCP proteins with dithionite without loss of diffraction quality. This paper reports the X-ray crystal structures of the reduced HCPs from *Dd* and *Dv*. Unprecedented large structural changes in the hybrid cluster are observed upon reduction and are rationalized with the enzyme's putative role as a reductase.

Materials and methods

Crystallization

The HCP from *Dd* was anaerobically purified as previously described [8]; the protein from *Dv* was obtained from a *D. vulgaris* clone overproducing HCP from the recombinant plasmid pJSP104 [9] and purified as for the *Dd* protein. Crystals of both HCPs were grown in a nitrogen environment inside a glove box system ($pO_2 < 1$ ppm) at different temperatures by the sitting drop vapour-diffusion method. For *Dd* crystallization, trials were set up at 279, 283 and 293 K, yielding needle-shaped pale yellow crystals in PEG 4000 (concentration range 25–35%) and MES (pH range 6.0–6.7). The best crystals grew at 279 K in 35% PEG 4000 and 0.1 M MES buffer at pH 6.5. Protein solution (1.5 μL, 12.6 mg mL^{-1} in 20 mM Tris-HCl, pH 7.6, and 0.2 M NaCl) and an equal amount of precipitant solution were allowed to equilibrate against 500 μL of the latter in the reservoir. Crystals took around 1 month to grow to a maximum size of approximately 0.2 mm×0.1 mm×0.08 mm.

For the *Dv* enzyme, crystallization trials at 277 K yielded rectangular-shaped laminar pale yellow crystals in PEG 4000 (concentration range 15–30%) and MES (pH range 6.0–6.5). The best crystals were obtained in 25% PEG 4000 and 0.1 M MES buffer at pH 6.5. A protein solution (2.0 μL, 25 mg mL^{-1} in

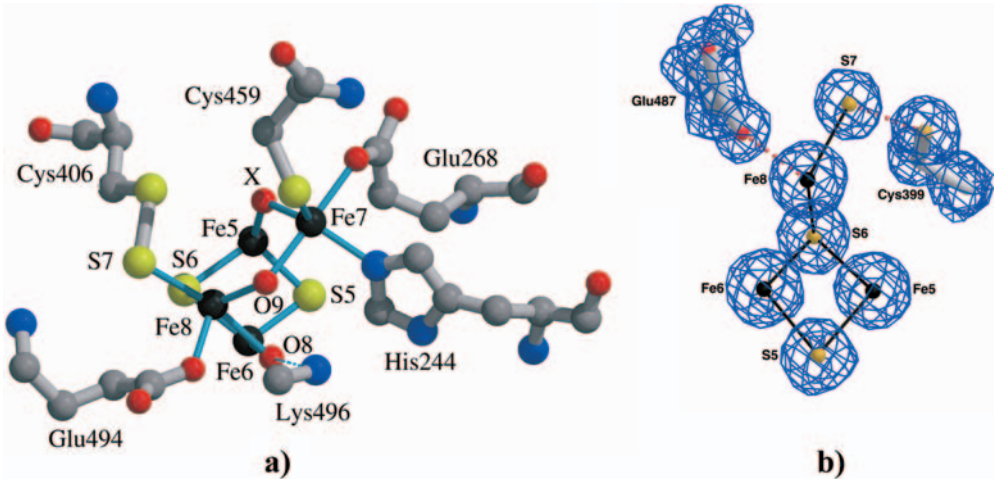

20 mM Tris-HCl at pH 7.6 and 0.05 M NaCl) and an equal amount of precipitant solution were allowed to equilibrate against 500 μL of the latter in the reservoir. Crystals took around 6 weeks to grow to a maximum size of 0.2 mm×0.2 mm×0.05 mm.

Reduction of the crystals

Crystals obtained as previously described were reduced by soaking with sodium dithionite. For *Dd*, a solution of 0.22 M $Na_2S_2O_4$ in freshly prepared mother liquor was added to drops containing crystals, resulting in an approximate final concentration of sodium dithionite in the drop of 0.18 M. For *Dv*, the same procedure was applied, but with a higher concentration of reducing agent, resulting in an approximate final concentration of sodium dithionite in the drop of 0.30 M. In both cases the crystals (previously cryo-protected by transfer to a solution obtained by adding 15% of glycerol to the mother liquor) were flash-cooled in liquid nitrogen after 2 hours soaking and stored. Addition of sodium dithionite to the drop and flash freezing were carried out inside the glove box system and all solutions used were de-aired under vacuum beforehand.

For *Dd*, the oxidation state of the crystals was tested by comparison of the UV-visible spectra measured from crystals in a microspectrophotometer [10] before and after reduction with sodium dithionite.

Assay for hydroxylamine reductase activity

Assays were performed under anaerobic conditions, in a Coy model a-2463 anaerobic chamber, using a Shimadzu UV-1203 spectrophotometer equipped with a stirring cell. A solution of hydroxylamine (1 M) adjusted to pH 7.0 was used in all assays. The assay mixture (1.2 mL), containing HEPES buffer (100 mM, pH 7.0), EDTA (10 μM) and methyl viologen (0.2 mM), was reduced with sodium dithionite until an absorbance at 600 nm ($\epsilon_{600} = 13\ mM^{-1}\ cm^{-1}$) close to 1 was obtained. Hydroxylamine was added (final concentration 100 mM) to the assay solution, and the reaction was started by the addition of HCP; no change in the activity was detected by changing the order of addition of the hydroxylamine or protein solutions. The pH-dependence assays for the NH_2OH reduction were also determined at pH 7.5 and 8.8, using Tris-HCl buffer (100 mM) adjusted to the desired pH. Activities are expressed as micromoles of NH_2OH reduced per minute per milligram of protein, taking into account that for the reduction of hydroxylamine, two equivalents of reduced methyl viologen are consumed.

Immuno-blotting

Immuno-blotting with antibodies against *D. vulgaris* HCP [1] was used to monitor the expression of the *Dd* HCP grown using either nitrate or sulfate as terminal electron acceptors.

X-ray data collection

The reduced form of the HCP from Dd

X-ray data were collected from a single cryo-cooled crystal at 100 K on beamline ID14-4 at the ESRF (Grenoble) synchrotron radiation source using a wavelength of 0.939 Å. The ADSC Q4R CCD detector was positioned at a distance of 100 mm from the sample and the beam size used was 30 μm × 30 μm. The effects of radiation damage were assessed using the individual frame *B*-factors referred to the first image and comparing images taken from identical ϕ rotation ranges at the start and end of the data collection; there appeared to be no significant radiation damage.

Data were processed using DENZO [11] and the indexed intensities were merged and converted to structure factors using the programs ROTAPREP, SCALA and TRUNCATE in the CCP4 program suite [12]. Details of data collection are given in Table 1.

Table 1 Data collection statistics

Data collection statistics	*Dd*	*Dv*
Beam line	ID14-4 (ESRF)	ID14-2 (ESRF)
Space group	*P*1	$P2_12121$
Z	2	1
Resolution(Å)	1.25	1.55
Highestres. shell (Å)	1.28–1.25	1.59–1.55
Wavelength(Å)	0.939	0.933
Cell dimensions		
a (Å)	57.75	64.05
b (Å)	61.99	67.46
c (Å)	72.80	134.95
α (°)	82.72	90.00
β (°)	73.74	90.00
γ (°)	87.44	90.00
Total no. of *hkl*	448,850	262,651
No. of batches/rotation angle (°)	360/0.5	425/0.2
Number of unique *hkl*	246,621	81,856
Average multiplicity[a]	1.8 (1.8)	3.2 (3.8)
R_{merge} ($\Sigma\|I - <I>\|/\Sigma <I>$)[a]	0.040 (0.098)	0.071 (0.254)
Average $I/\sigma(I)$[a]	7.8 (3.6)	13.2 (3.6)
% completeness[a]	92.7 (78.7)	95.7 (93.5)
Average B(Wilson) (Å)^2	7.1	19.3

[a]Values in parentheses refer to highest resolution shell

The asymmetric unit (equivalent to the unit cell for space group *P*1) accommodates two molecules of molecular weight 60 kDa, corresponding to a V_m of 2.03 Å^3 Da^{-1} [13] and a solvent content of some 39%.

The reduced form of the HCP from Dv

X-ray data were collected from a single cryo-cooled crystal at 100 K on beamline ID14-2 at the ESRF (Grenoble), using a wavelength of 0.933 Å and an ADSC Q4R CCD detector placed at a distance of 120 mm from the sample; the beam size used was 25 μm × 25 μm. Radiation damage effects were assessed in a similar manner to that used for *Dd* and again there appeared to be no significant radiation damage. The diffraction data were also processed as for *Dd* and details are given in Table 1.

The asymmetric unit accommodates only one molecule of *Dv*, corresponding to a V_m of 2.04 Å^3 Da^{-1} [13] and a solvent content of some 40%.

Structure solution

The reduced form of the HCP from Dd: *ab initio phasing*

The ab initio phasing program ACORN [14] was used to generate preliminary experimental phases. The *E*-values (normalized structure factors) required by ACORN were generated from the SCALA output using the CCP4 [12] program ECALC. No reflections were excluded in the calculation of *E*-values. In ACORN the initial phases are generated from a fragment, such as a set of heavy atoms, with a previously determined position. It was assumed that the [4Fe-4S] cubane clusters, one in each monomer in the asymmetric unit, would be geometrically identical and in the same position in the unit cell in the reduced and oxidized forms of the HCP protein. Increasing numbers of iron atoms from the two cubane clusters in the asymmetric unit of the as-isolated *Dd* anaerobic structure at 1.25 Å resolution (PDB code 1GNL) were used as a starting fragment until successful phasing of the structure was accomplished. In all cases, default settings for ACORN were used and details of the phasing are given in the Supplementary material. For

this particular protein and at this resolution, a clearly interpretable electron density map was obtained using all of the eight iron atoms from the cubane clusters of both monomers. However, a second run with only six Fe atoms in the cluster also gave a positive result, albeit with a significant increase in computational time. In both cases, only the cubane cluster iron atoms were used in order to minimize any possible bias in the resulting electron density map; no assumptions were made concerning the nature of the hybrid clusters.

The initial Fourier map was of high quality and clearly showed electron density consistent with the two molecules of the *Dd* protein in the asymmetric unit. In each molecule, nearly all the main chain and side chain residues could be positioned directly. However, in the hybrid cluster, large positional changes were evident for both Fe8 and the persulfide S atom to which it is attached in the oxidized form of the protein. Figures 1b and 2b compare the electron density at the hybrid cluster in the as-isolated and reduced forms of the HCP from *Dd*. The [2Fe-2S] moiety was also slightly moved with respect to the oxidized as-isolated protein and there were no indications of any bridging oxygen atoms in the hybrid cluster.

The reduced form of the HCP from Dv

Since the resolution, 1.55 Å, was not sufficient for ab initio phasing, an alternative molecular replacement procedure was used, as described by Perrakis et al. [15]. The structure of the anaerobically as-isolated protein at 1.35 Å resolution (unpublished results) was used to generate phase information and the resulting data interpreted by ARP/wARP [16].

Structure refinement

The reduced form of HCP from Dd *at 1.25 Å resolution*

Refinement was performed using the maximum likelihood function implemented in REFMAC [17], starting with the model determined for *Dd* at 1.25 Å resolution [8], but with new positions for Fe8 and S7 and no bridging oxygen atoms in the hybrid cluster. At this stage, no solvent molecules were included. Rounds of conjugate gradient sparse matrix refinement with bulk solvent modelling according to the Babinet principle [18] were alternated with model building using the O program [19] in combination with SigmaA-weighted $2|F_o| - |F_c|$ and $|F_o| - |F_c|$ electron density maps [20].

For the hybrid clusters, attempts were made to refine the Fe8 atoms as sulfur and the S7 as oxygen, but these resulted in anomalously small temperature coefficients, indicating that the assignment of Fe and S respectively was correct. The assignment was also verified using anomalous dispersion techniques. The geometries of the cluster atoms were unrestrained throughout the refinement, and in the final stages all the Fe and S atoms (inorganic S and cysteine S) associated with the two clusters in each molecule were allowed to refine anisotropically. After the first round of refinement, solvent molecules were added to the model based on standard geometrical and chemical restraints; they were subsequently deleted if their isotropic thermal coefficients exceeded 50 $Å^2$ or they were not visible at the 0.8 rms level in SigmaA-weighted $2|F_o| - |F_c|$ electron density maps. In several regions, solvent molecules were close together, indicating either partially occupied sites or possible stretches of poly(ethylene glycol) density. Where solvent peaks occurred within 2.0 Å of one another, they were treated as partially occupied sites with occupancies (not refined) roughly proportional to the peak volumes. In addition to the solvent peaks assigned to water, there were two regions of density that were clearly different to the normal solvent structure. The first of these lay in the vicinity of the cubane cluster in molecule A. It was unclear what it represented, but, for example, the density could accommodate a dithionite anion (DTN). This was considered reasonable since dithionite was used in the protein reduction process. If this were the case, one oxygen atom of the anion would have a closest approach of about 7.0 Å to Fe3 in the cubane cluster; the remaining oxygens of the anion would form hydrogen bonds with neighbouring solvent molecules. However, attempts to refine this moiety indicated that if dithionite was present, then the occupancy was only around 0.5. The density did not appear to be present near to the cubane cluster in molecule B. The second region of density lay between molecules A and B in the asymmetric unit. Although the density was not completely contiguous, it could clearly be ascribed to a MES molecule; 0.1 M MES buffer was used in the crystallization process. One of the sulfite oxygen atoms interacts with the side chain of Lys313 in molecule B. A second interacts with the main chain amino atom of Asp314, also in molecule B, and with a neighbouring solvent molecule, whilst the third interacts with a solvent molecule only. The morpholino moiety fits into a pocket in molecule A in the vicinity of Lys434.

For the protein, hydrogen atoms were included as "riding" atoms. Details of the final refinement statistics are given in Tables 2 and 3. Several residues were modelled in more than one conformation. A number of the surface residue side chains, particularly lysines, had no visible electron density after the CG atom, but as far as possible these were modelled in geometrically feasible positions. Details are shown in Table 2.

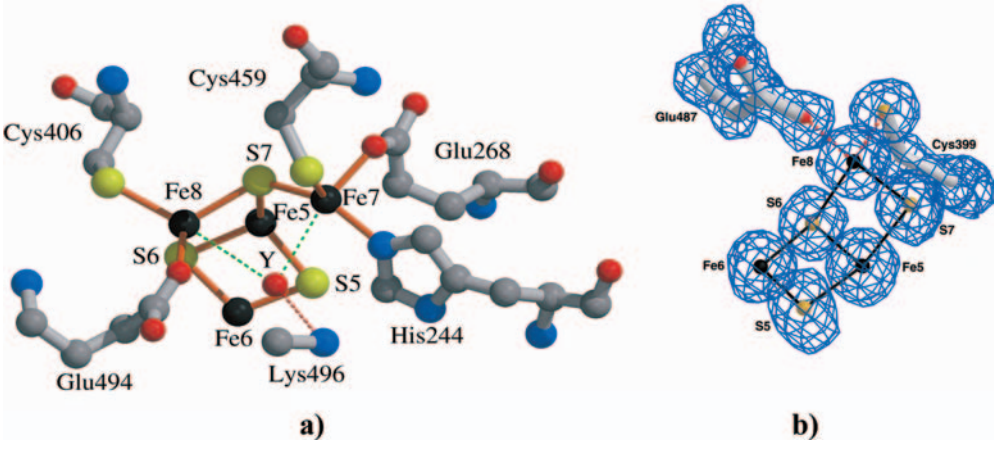

Fig. 2 **a** A model representation of the hybrid cluster in the reduced form of *Dv* (PDB ID 1OA1), showing moiety Y between the positions previously occupied by O8 and O9. Residues Cys434 and Cys312, bound to Fe5 and Fe6, respectively, have been omitted for clarity. **b** Electron density at the reduced hybrid cluster in *Dd* (PDB ID 1OA0). The contour level is 1.0 rms in a SigmaA-weighted $2|F_o| - |F_c|$ Fourier synthesis. The SG atom of Cys399 is directly bound to Fe8 and S7 has moved towards the X position in the as-isolated enzyme, and is bound to Fe5, Fe7 and Fe8. This is a different orientation to **a** and Fe7 and its environment have been omitted for clarity

Table 2 Refinement statistics for reduced HCPs from *Dd* and *Dv* at resolutions of 1.25 Å and 1.55 Å, respectively

	Dd	*Dv*
PDB ID	1OA0	1OA1
Amino acids	2×544	1×553
Protein atoms	4176 A; 4181 B	4252
Solvent atoms	2044	866
No. in dual conformations	173	–
Other atoms	2×16 + 1×DTN + 1×MES	1×16 + 2×GOL
Resolutionlimits (Å)	29.49 – 1.25	19.50 – 1.55
Working set *R* (observations)	0.131 (240,495)	0.131 (73,710)
Test set *R* (observations)	0.148 (6123)	0.153 (4074)
Highest resolution shell		
R (obs)	0.150 (14,346)	0.168 (5497)
Free *R* (obs)	0.166 (365)	0.199 (295)
Cruickshank's DPI [32] (Å)	0.038	0.072
Average B_{iso} (Å^2)		
All atoms	11.9	15.1
Protein atoms	8.1 A; 8.6 B	12.4
Main chain	7.3 A; 7.8 B	11.3
Side chain	8.8 A; 9.5 B	13.5
Solvent	25.3	29.2
Residues not found	G544 A and B	–
Residues in alternative conformations	A: K16, V21, R61, M90, K165, N168, M174, N232, G282,E296, V302, V310, S345, I347, E364, K404, E372, N528	D109, I151, R171, T173, E335, K338, E390, K411,N443
		GOL1
	B: V21, D59, R64, M90, S117, N168, M174, M206,K281, K292, E296, V302, V310, I338,E340, S345, K404, K418, I483, Q526,I529	
Residues not complete	A: K521, E525	–
	B: N436	–
Distance deviations[a]		
Bond distances (Å)	0.008	0.011
Bond angles (°)	1.245	1.292
Plana rgroups (Å)	0.006	0.006
Chiral volume deviation (Å^3)	0.138	0.090

[a]rms deviations from standard values

The reduced form of the HCP from Dv *at 1.55 Å resolution*

Refinement was also performed using the maximum likelihood function implemented in REFMAC, starting with the model produced by ARP/wARP, but inserting atoms one at a time for the hybrid cluster; no solvent structure was included in the initial stages. Rounds of conjugate gradient sparse matrix refinement with bulk solvent modelling according to the Babinet principle were alternated with model building using XtalView [21] in combination with SigmaA-weighted electron density syntheses.

In a similar manner to the *Dd* protein, attempts were made to refine the Fe8 atom in the hybrid cluster as sulfur and the S7 atom as oxygen, but again these resulted in anomalously small thermal coefficients, suggesting that the original assignments were correct. Density in the solvent region, although not completely contiguous, could be clearly ascribed to two glycerol molecules; 25% glycerol buffer was used as a cryo-protector. Further details of the refinement are given in Tables 2 and 3.

Quality of the refined structures

The quality of the refined structure of *Dd* is high, with final values for *R* and R_{free} of 13.1% and 14.8%, respectively, and an overall *G* factor of 0.21 [22] (Table 3). As in the oxidized structure, two residues in each monomer, Ser263 and Asn299, lie in the disallowed region of the Ramachandran plot [23]. In all cases, these residues lie in well-defined density at bends between helices and strands.

Table 3 Quality of reduced HCP structures

	Dd	*Dv*
Overall *G* factor[a]	0.21	0.20
Ramachandran analysis (%) (no.)[a]		
Favourable	93.7 (888)	94.1 (450)
Additional	5.6 (53)	5.6 (27)
Generous	0.3 (3)	0 (0)
Disallowed	0.4 (4)	0.2 (1)
No. of glycine residues	2×49	50
No. of proline residues	2×18	23

[a]G factor and Ramachandran analysis were determined by PROCHECK [22]

The quality of the refined structure of *Dv* is also high, with final *R* and R_{free} values of 13.1% and 15.6%, respectively, and an overall *G* factor of 0.19. Residue Asn303 (equivalent to Asn 299 in *Dd*) lies in the disallowed region of the Ramachandran plot, but the density is very well defined.

Figures 1, 2, 3, 4 were produced with the help of the programs Molscript [31], Bobscript [32] and Raster3D [33].

Information for the two data sets and the associated structures has been deposited in the Protein Data Bank [24] with deposition codes 1OA0 and 1OA1 for *Dd* and *Dv*, respectively.

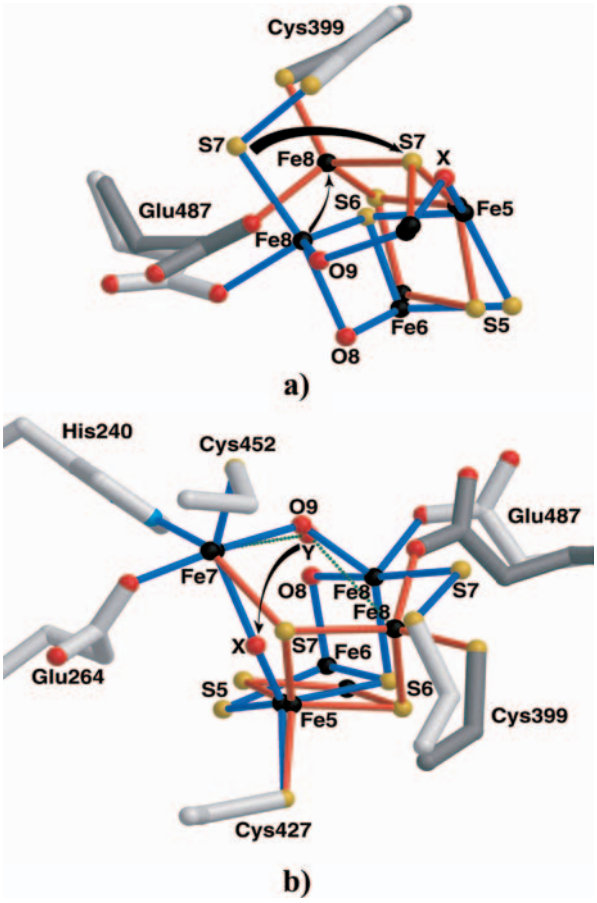

Fig. 3a, b Superposition of the as-isolated oxidized and reduced clusters in *Dd*. The as-isolated oxidized form is in *blue* and the reduced form in *red*. The superposition was achieved using the LSQ option in the O program suite [19] and rotating and translating the whole of the molecule from the asymmetric unit of *Dv* onto molecule A in the asymmetric unit of *Dd*. **a** A view from the top of the [2Fe-2S] moiety comprising Fe5 and Fe6. For clarity, residues Cys427 (bound to Fe5), Cys308 (Fe6) and His240, Glu264 and Cys452 (Fe7) have been omitted, as well as the Y site in the reduced protein. **b** A view almost parallel to the plane defined by the [2Fe-2S] moiety. Residue Cys308 (bound to Fe6) has been omitted for clarity

Results and discussion

The overall architecture of the reduced forms of the HCP proteins prepared anaerobically from *Dd* and *Dv* is almost identical to that of the as-isolated oxidized forms, prepared both anaerobically {[8] (*Dd*), unpublished results (*Dv*)} and aerobically {[7] (*Dv*)}. Each molecule contains three domains and two iron-sulfur clusters; one cluster is a conventional cubane cluster situated at the N-terminus of domain 1, and the hybrid cluster is located at the interface of the three domains. It is in this hybrid cluster that the major differences between the reduced and oxidized forms of the protein occur. Throughout this discussion the atom and residue numbering scheme appropriate to *Dd* will be utilized. Geometrical parameters cited for *Dd* are the average values for the A and B molecules in the asymmetric unit.

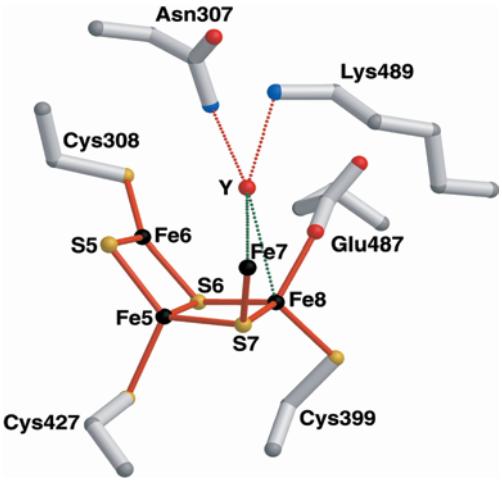

Fig. 4 The environment of site Y in the reduced form of the hybrid cluster in *Dd*. Y has been modelled as an oxygen/hydroxide and, in this case, can form hydrogen bonds with the side chains of Lys489 and Asn307. The previous position for X, in the as-isolated oxidized form, is now occupied by a well-refined sulfur atom, S7. Residues His240, Glu264 and Cys452 bound to Fe7 have been omitted for clarity

Thus, in the hybrid cluster of the reduced protein the Fe7 atom linked to the protein through residues His240, Glu264 and Cys452 is virtually unchanged in position, the [2Fe-2S] moiety involving Fe5 and Fe6 and linked to the protein through cysteine residues 427 and 308 respectively is slightly tilted, but Fe8 and S7 of the persulfide moiety at Cys399 undergo large movements in position and coordination. Concomitantly, residues Cys399 and Glu487, attached to Fe8, also undergo significant positional changes. Figures 1a and 2a show the arrangement of the atoms in the hybrid cluster for the as-isolated and reduced forms of the HCP from *Dv*. Figure 3 highlights the almost identical changes for the HCP from *Dd* by the superposition of the as-isolated and reduced forms of the hybrid cluster.

The persulfide S atom, S7, moves very close to the position of atom X, defined as an oxygen atom or OH^- anion in the as-isolated form of the protein, and appears to replace it. Thus, S7 forms the second side of a cube in conjunction with atoms Fe5, Fe8 and S6 and is only 2.4 Å from Fe7. The movement of S7 in *Dd* is 3.6 Å and the SG of Cys399 now forms a direct bond to Fe8. In turn, Fe8 has moved by some 2.1 Å. The geometries of the iron atoms in the reduced form of the hybrid cluster can now be described as tetrahedral for Fe5, Fe7 and Fe8 and trigonal planar for Fe6, in sharp contrast to those observed in the as-isolated oxidized cluster. Table 4 compares Fe-Fe, Fe-S and other important distances in the as-isolated, oxidized and reduced forms of the HCP proteins.

The hybrid cluster in the reduced form of the protein also lacks the μ-bridging oxygen atoms O8 and O9 between Fe6 and Fe8 and between Fe7 and Fe8, respectively, present in the as-isolated form. However, there is a peak in the electron density of the reduced

Table 4 Geometry (bond distances in Å) of the cubane and hybrid clusters in the as-isolated oxidized and reduced HCP proteins from *Dd* and *Dv*.

PDB ID	*Dd* (A) as-isolated 1GNL	*Dd* (B) as-isolated	*Dd* (A) reduced 1OA0	*Dd* (B) reduced (unpublished results)	*Dv* as-isolated 1OA1	*Dv* reduced
(a) Hybrid cluster						
Fe1–Fe2	2.73	2.73	2.74	2.74	2.74	2.71
Fe1–Fe3	2.69	2.70	2.71	2.71	2.70	2.70
Fe1–Fe4	2.77	2.76	2.79	2.79	2.78	2.79
Fe1–S1	2.30	2.31	2.30	2.32	2.32	2.27
Fe1–S2	2.29	2.28	2.31	2.30	2.26	2.30
Fe1–S3	2.32	2.33	2.34	2.33	2.33	2.32
Fe1–Cys6 SG	2.28	2.29	2.32	2.32	2.29	2.27
Fe2–Fe3	2.71	2.72	2.72	2.71	2.69	2.69
Fe2–Fe4	2.69	2.70	2.69	2.69	2.66	2.64
Fe2–S1	2.28	2.26	2.30	2.29	2.29	2.26
Fe2–S2	2.36	2.35	2.37	2.36	2.34	2.31
Fe2–S4	2.32	2.33	2.34	2.32	2.32	2.33
Fe2–Cys9 SG	2.26	2.26	2.28	2.29	2.27	2.31
Fe3–Fe4	2.73	2.74	2.75	2.75	2.71	2.69
Fe3–S1	2.33	2.34	2.34	2.36	2.33	2.33
Fe3–S3	2.32	2.32	2.35	2.33	2.33	2.31
Fe3–S4	2.27	2.27	2.30	2.29	2.27	2.27
Fe3–Cys18 SG	2.31	2.30	2.33	2.33	2.36	2.32
Fe4–S2	2.36	2.34	2.37	2.37	2.33	2.34
Fe4–S3	2.26	2.26	2.30	2.29	2.28	2.28
Fe4–S4	2.34	2.35	2.36	2.37	2.35	2.32
Fe4–Cys24 SG	2.30	2.29	2.34	2.30	2.31	2.31
(b) Hybrid cluster						
Fe5–Fe6	2.76	2.77	2.76	2.76	2.75	2.73
Fe5–Fe7	3.63	3.67	3.98	3.97	3.64	3.89
Fe5–Fe8	3.35	3.36	2.84	2.84	3.12	2.79
Fe5–S5	2.31	2.31	2.31	2.30	2.31	2.28
Fe5–S6	2.32	2.31	2.35	2.33	2.30	2.35
Fe5–S7	–	–	2.34	2.35	–	2.29
Fe5–Cys427 SG	2.32	2.33	2.36	2.36	2.32	2.34
Fe5–X	2.00	1.99	–	–	1.94	–
Fe6–Fe7	4.94	4.86	5.60	5.58	5.12	5.57
Fe6–Fe8	3.02	3.02	3.79	3.78	3.15	3.74
Fe6–S5	2.25	2.25	2.22	2.22	2.19	2.22
Fe6–S6	2.27	2.26	2.22	2.21	2.25	2.23
Fe6–Cys308 SG	2.33	2.33	2.30	2.31	2.31	2.28
Fe6–O8	1.98	1.93	–	–	2.11	–
Fe6–Y	–	–	3.81	3.80	–	4.00
Fe7–Fe8	3.55	3.56	4.13	4.11	3.37	4.11
Fe7–S7	>4.5	>4.5	2.35	2.35	>4.5	2.34
Fe7–His240 NE2	2.13	2.16	2.18	2.17	2.18	2.12
Fe7–Glu264 OE2	2.15	2.16	2.08	2.09	2.16	2.06
Fe7–Cys452 SG	2.45	2.42	2.35	2.37	2.45	2.34
Fe7–O9	2.13	2.14	–	–	2.17	–
Fe7–X	2.06	2.08	–	–	2.10	–
Fe7–Y	–	–	3.14	3.15	–	2.78
Fe8–S6	2.42	2.44	2.35	2.34	2.42	2.29
Fe8–S7	2.54	2.54	2.36	2.36	2.56	2.35
Fe8–Cys399 SG	–	–	2.36	2.35	–	2.32
Fe8–Glu487 OE2	2.04	2.02	2.07	2.07	2.09	2.01
Fe8–O8	2.19	2.17	–	–	2.24	–
Fe8–O9	1.93	1.95	–	–	1.89	–
Fe8–X	3.31	3.33	–	–	3.26	–
Fe8–Y	–	–	3.44	3.41	–	3.33
S7–Cys399 SG	2.09	2.09	4.06	4.04	2.10	4.00
O8–Asn307 ND2	3.02	3.04	–	–	2.88	–
O9–Lys489 NZ	2.99	2.95	–	–	2.95	–
Y–Asn307 ND2	–	–	3.14	3.13	–	3.29
Y–Lys489 NZ	–	–	2.89	2.88	–	2.93

[a]Residue numbering refers to the *Dd* protein. The values for the as-isolated *Dd* protein are from [8]; values for the as-isolated *Dv* protein are unpublished results at a resolution of 1.35 Å

[b]We estimate using the Cruickshank method [31,32] that the estimated uncertainties in the bond lengths involving Fe and S are less than 0.03 Å and 0.02 Å for *Dd* and *Dv*, respectively

protein, Y, not present in the as-isolated form and roughly in between the positions formerly occupied by O8 and O9, as shown in Fig. 4. Y has been refined as a single oxygen atom (OH^-), but the electron density at the 1 rms level is not spherical and could possibly accommodate a di-atomic (in a similar manner to X in the as-isolated protein) or even tri-atomic species. Y is some 3.1 Å and 3.4 Å from Fe7 and Fe8, respectively, too long for a direct bond. It is, however, well within hydrogen bonding range of the NZ of Lys489 (2.9 Å) and the ND2 of Asn307 (3.1 Å); both these residues are conserved in most of the known HCP sequences.

It is likely that the significant structural changes between the as-isolated (prepared anaerobically or aerobically) and reduced forms of the HCP proteins reflect their function, which nevertheless remains to be established. In the cases of *Escherichia coli* and *Morganella morganii*, two facultative anaerobes, expression of HCP was only observed when these bacteria were grown in nitrate or nitrite as terminal electron acceptors. This suggested a role for HCPs in the metabolism of nitrogen oxides in these organisms [1]. For another facultative anaerobe, *Shewanella oneidensis*, an increase in the expression of HCP was also observed when the cells were grown in nitrate as electron acceptor, as compared with the expression in aerobically grown cells [2]. However, disruption of the HCP gene in either *E. coli* or *M. morganii* had no effect on anaerobic cell growth, in the presence of nitrate or nitrite (minimal or rich media) [1]. In the case of *D. desulfuricans* ATCC 27774, using antibodies against *Dv* HCP, immuno-blotting of cells showed only a small increase in the expression of *Dd* HCP when the cells were grown in the presence of sulfate/nitrate mixes (Fig. 5, lanes 2–4). In addition, for both *Dv* and *Dd*, HCP is still expressed in significant amounts when the cells are grown using sulfate as the only terminal electron acceptor (Fig. 5, lane 1).

Furthermore, genes encoding HCP proteins are present in the genomes of a wide variety of organisms that are not involved in the biological nitrogen cycle (for example, *Thermotoga maritima* and *Pyroccocus furiosus*), and present quite variable genomic organizations. Thus, at the present stage, it is not clear whether HCPs are directly involved in the metabolism of nitrogen species.

Quite recently, Wolfe et al. [3] reported that the recombinant HCP from *E. coli* exhibits in vitro hydroxylamine reductase activity, again suggesting a link of this protein to nitrogen metabolism. Such reductase activity can be rationalized by the structural changes undergone by the HCP enzymes as they transform from the reduced state to the as-isolated oxidized state. Thus, it can be envisaged that the substrate will initially bind to the reduced form of the enzyme close to the position of Y. Reduction of the substrate, with concomitant oxidation of the enzyme, will then take place as the substrate moves from the Y position to the X position in the as-isolated oxidized form. The product will then diffuse away from the active site and eventually

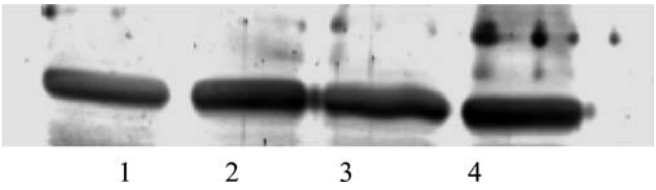

Fig. 5 Immuno-blotting, using a polyclonal antibody against *Dv* HCP, of *D. desulfuricans* ATCC 27774 cell extracts from cultures grown with sulfate, nitrate and combinations of the two. The lanes contain lysates of equal amounts of *D. desulfuricans* ATCC 27774 cells grown in Saunders medium with lactate and 50 mM sulfate (*lane 1*), 50 mM sulfate + 50 mM nitrate (*lane 2*), 50 mM sulfate + 10 mM nitrate (*lane 3*) and 50 mM nitrate (*lane 4*). Only a small increase in the expression of *Dd* HCP is observed when the cells were grown in the presence of nitrate (*lane 4*)

away from the enzyme through the extensive hydrophobic cavity that gives ready access to the hybrid cluster [7]. The large movement of S7 will not only make accessible the X position in the oxidized form of the enzyme, but it may also assist in the electron transfer process. The possibility also exists that this sulfur atom may even provide an "S-Y" intermediate to assist in the translocation of the substrate at Y to the product at X.

However, in the present work, hydroxylamine reductase activity measurements have been performed for the anaerobically purified *Dd* HCP (see Materials and methods). The specific activity determined, 3.6 μmol NH_2OH reduced min^{-1} mg^{-1}, is approximately 10 times lower than that reported for the *E. coli* recombinant enzyme, and independent of pH between pH 7.0 and 8.8. It should be noted that hydroxylamine is quite unstable at basic pH [25]. The turnover value for the *E. coli* HCP (ca. 40 s^{-1}) should also be compared with those from other *E. coli* enzymes known to reduce hydroxylamine, albeit having nitrite as their main physiological substrate. Thus, for the periplasmic pentaheme nitrite reductase and the cytoplasmic siroheme-containing nitrite reductase, expressed under nitrate and nitrite respiring conditions, this is reflected in high K_M values for hydroxylamine, in the millimolar range, compared with the micromolar K_M values for nitrite. The pentaheme nitrite reductase has, at neutral pH, a turnover for hydroxylamine reduction almost 50-fold higher than HCP (2380 s^{-1} [26]); values for the *E. coli* cytoplasmatic enzyme could not be found in the literature, but very similar siroheme-containing enzymes, the spinach nitrite reductase and the *E. coli* sulfite reductase, have turnovers of about 500–750 s^{-1} [27, 28]. These facts, together with the very high K_M for the *E. coli* HCP (30 mM at neutral pH), therefore argue against a real physiological role of HCPs as hydroxylamine reductases.

The hybrid cluster in HCPs exhibits a complex redox behaviour and four redox reactions can be detected by, for example, EPR titration. On the basis of the differences in structures of the as-isolated oxidized and fully reduced proteins, which reveal the reduction of the Cys399 persulfide moiety, it cannot be excluded that at

least one of the EPR-detected transitions is due to this process, and not to a reduction based on the iron atoms in the cluster.

In conclusion, although the crystallographic studies alone cannot precisely define the natures of X and Y, the changes observed in the structure of the hybrid cluster as it transforms between the reduced and oxidized states give strong credence to the role of the HCPs as reductases. What is clearly indicated, by the structural changes in the HCPs in moving from the reduced to the oxidized states, is that the enzyme acquires two bridging oxygen atoms. Another possible function for the enzyme could be to sequester oxygen and/or its by-products (eventually together with reactive nitrogen species) in an anaerobic environment. That is, the HCP could protect the organisms against oxidative stress [4] or against reactive nitrogen species. Further biochemical, spectroscopic and crystallographic studies are in progress to examine these hypotheses.

Acknowledgements We thank the European Synchrotron Radiation Facility, Grenoble, France, and the staff of the Macromolecular Crystallography Group for the provision of synchrotron radiation facilities, without which the high-resolution studies would not have been possible. The ESRF also provided a PhD studentship for S.M. and kindly provided partial support for D.G.A. D.G.A. also acknowledges a grant from Fundação para a Ciência e Tecnologia (FCT), SFRH (BD/6480/2001). C.V.R. acknowledges a grant from Praxis XXI (BD/19879/99). P.F.L. would like to acknowledge the assistance and cooperation of the Department of Crystallography, Birkbeck College, University of London, UK. This work was partially funded by FCT, SAPIENS (POCTI/BME/38859/2001). The authors would also like to thank to Dora Alves for her valuable help on some aspects of *Dv* protein purification. Figures 1 to 4 were produced with the help of the programs Molscript 28, Bobscript 29and Raster 3D 30

References

1. van den Berg WAM, Hagen WR, van Dongen WMAM (2000) Eur J Biochem 267:666–676
2. Beliaev AS, Thompson DK, Khare T, Lim H, Brandt CC, Li G, Murray AE, Heidelberg JF, Giometti CS, Yates J III, Nealson KH, Tiedje JM, Zhou J (2002) J Integrative Biol 6: 39–60
3. Wolfe MT, Heo J, Garavelli JS, Ludden PW (2002) J Bacteriol 184:5898–5902
4. Briolat V, Reysset G (2002) J Bacteriol 184:2333–2343
5. Dobbek H, Svetlitchnyi V, Gremer L, Huber R, Meyer O (2001) Science 293:1281–1285
6. Arendsen AF, Hadden J, Card G, McAlpine AS, Bailey S, Zaitsev V, Duke EHM, Lindley PF, Kröckel M, Trautwein AX, Feiters MC, Charnock JM, Garner CD, Marritt SJ, Thomson AJ, Kooter IM, Johnson MK, van den Berg WAM, van Dongen WMAM, Hagen WR (1998) J Biol Inorg Chem 3:81–95
7. Cooper SJ, Garner CD, Hagen WR, Lindley PF, Bailey S (2000) Biochemistry 39:15044–15054
8. Macedo S, Mitchell EP, Romão CV, Cooper SJ, Coelho R, Liu MY, Xavier AV, LeGall J, Bailey S, Garner CD, Hagen WR, Teixeira M, Carrondo MA, Lindley PF (2002) J Biol Inorg Chem 7:514–525
9. Stokkermans JPWG, Pierik AJ, Wolbert RBG, Hagen WR, van Dongen WMAM, Veeger C (1992) Eur J Biochem 208:435–442
10. Bourgeois D, Vernede X, Adam V, Fioravanti E, Ursby T (2002) J Appl Crystallogr 35:319–326
11. Otwinowski Z, Minor W (1997) Methods Enzymol 276:307–326
12. Collaborative Computational Project Number 4 (1994) Acta Crystallogr Sect D 50:760–763
13. Matthews BW (1968) J Mol Biol 33:491–497
14. Foadi J, Woolfson MM, Dodson EJ, Wilson KS, Jia-xing Y, Chao-de Z (2000) Acta Crystallogr Sect D 56:1137–1147
15. Perrakis A, Harkiolaki M, Wilson KS, Lamzin VS (2001) Acta Crystallogr Sect D 57:1445–1450
16. Lamzin VS, Perrakis A, Wilson KS (1999) In: Rossmann M, Arnold E (eds) International tables for crystallography; crystallography of biological macromolecules. Kluwer, Dordrecht, pp 720–722
17. Murshudov GN, Vagin AA, Dodson EJ (1997) Acta Crystallogr Sect D 53:240–255
18. Tronrud D (1996) In: Dodson E, Moore M, Ralph A, Bailey S (eds) Macromolecular refinement. Proceedings of CCP4 study weekend. Daresbury Laboratory, Warrington, UK, pp 1–10
19. Jones TA, Zou JY, Cowan SW, Kjeldgaard M (1991) Acta Crystallogr Sect A 47:110–119
20. Read RJ (1986) Acta Crystallogr Sect A 42:140–149
21. McRee DE (1992) J Mol Graph Model 10:44–46
22. Laskowski RA, MacArthur MW, Moss DS, Thornton JM (1993) J Appl Crystallogr 26:283–291
23. Ramakrishnan C, Ramachandran GN (1965) Biophys J 5:909–933
24. Berman HM, Westbrook J, Feng Z, Gilliland G, Bhat TN, Weissig H, Shindyalov IN, Bourne PE (2000) Nucleic Acids Res 28:235–242
25. Greenwood NN, Earnshaw A (1994) Chemistry of the elements, 2nd edn. Pergamon, Oxford, pp 494–496
26. Bamford VA, Angove HC, Seward HE, Thomson AJ, Cole JA, Butt JN, Hemmings AM, Richardson DJ (2002) Biochemistry 41:2921–2931
27. Krueger RJ, Siegel LM (1982) Biochemistry 21:2892–2904
28. Siegel LM, Rueger DC, Barber MJ, Krueger RJ, Orme-Johnson NR, Orme-Johnson WH (1982) J Biol Chem 257:6343–6350
29. Kraulis PJ (1999) J Appl Crystallogr 24:946–950
30. Esnouf RM (1999) Acta Crystallogr Sect D 55:938–940
31. Merritt EA, Bacon DJ (1997) Methods Enzymol 277:505–524
32. Cruickshank DWJ (1996) In: Dodson E, Moore M, Ralph A, Bailey S (eds) Macromolecular refinement. Proceedings of the CCP4 study weekend. Daresbury Laboratory, Warrington, UK, pp 11–22
33. Cruickshank DWJ (1998) Acta Crystallogr Sect D 55:583–601